Copper doped $EuMnO_3$: Synthesis, Structure and Magnetic Properties

Aimei Yang,[1] Yunhan Sheng,[3] Mahammad Asim Farid,[2] Hao Zhang,[2] Xiaohuan Lin,[2] Guobao Li[2,*], Laijun Liu,[1,*]

Fuhui Liao,[2] Jianhua Lin[2,*]

[1]College of Materials and Engineering, Institution Guangxi Guilin University of Technology, Guilin 541004, China

[2]Beijing National Laboratory for Molecular Sciences, State Key Laboratory of Rare Earth Materials Chemistry and Applications, College of Chemistry and Molecular Engineering, Peking University, Beijing 100871, P. R. China

[3]The second high school attached to Beijing Normal University

1. Rietveld refinement details of the X-ray diffraction data for C1, C2, C3, C4, C5, and C6

Table S1 Rietveld refinement details of the X-ray diffraction data for C1, C2, C3 and C4 in *Pnma*

	C1	C2	C3	C4
Lattice parameter (Å)	a=5.8170(2), b=7.4763(2), c=5.3357(2)	a=5.7894(2), b=7.4737(2), c=5.3393(2)	a=5.7504(2), b=7.4721(2), c=5.3432(2)	a=5.7079(2), b=7.4706(2), c=5.3468(2)
Atom	x, y, z	x, y, z	x, y, z	x, y, z
Eu	0.0770(3), 0.2500(3), 0.9839(2)	0.0756(3), 0.2500(3), 0.9823(3)	0.0724(4), 0.2500(2) 0.9830(1)	0.0692(3), 0.2500(3), 0.9833(3)
Cu/Mn[a]	0.0000, 0.0000, 0.5000	0.0000, 0.0000, 0.5000	0.0000, 0.0000, 0.5000	0.0000, 0.0000, 0.5000
O1	0.4815(3), 0.2500(3), 0.0987(3)	0.4836(2), 0.2500(2), 0.0951(2)	0.4759(3), 0.2500(3), 0.1073(3)	0.4737(2), 0.2500(2), 0.1054(8)
O2	0.3209(3), 0.0442(3), 0.7251(3)	0.3145(3), 0.0442(2), 0.7213(3)	0.3180(3), 0.0479(3), 0.7325(3)	0.3135(3), 0.0507(2), 0.7267(3)
R factor[b]	R_{wp}=0.018, R_p=0.011	R_{wp}=0.018, R_p=0.011	R_{wp}=0.017, R_p=0.010	R_{wp}=0.020,R_p=0.012

[a]The occupancy of Cu/Mn is 0.000/1.000 for C1, 0.100/0.900 for C2, 0.200/0.800 for C3, and 0.300/0.700 for C4 .

[b] R_p is $\mathrm{sum}(|I_0-I_C|)/\mathrm{sum}(I_0)$, and R_{wp} is weighted R factors for X-ray diffraction data.

Table S2 Rietveld refinement details of the X-ray diffraction data for C5 and C6

	C5	C6
Phase 1	$EuMn_{1-x}Cu_xO_{3-\delta}$	$EuMn_{1-x}Cu_xO_{3-\delta}$
Space group	*Pnma*	*Pnma*
Lattice parameter (Å)	a= 5.7053(3), b= 7.4704(3), c= 5.3475(3)	a=5.7046(3), b= 7.4702(3), c= 5.3473(3)
Atom	x, y, z	x, y, z
Eu	0.0692(3), 0.2500(3), 0.9833(3)	0.0692(3), 0.2500(3), 0.9833(3)
Cu/Mn[a]	0.0000, 0.0000, 0.5000	0.0000, 0.0000, 0.5000
O1	0.4737(3), 0.2500(3), 0.1054(3)	0.4737(3), 0.2500(3), 0.1054(3)
O2	0.3135(3), 0.0507(3), 0.7267(3)	0.3135(3), 0.0507(3), 0.7267(3)
Phase 2	Eu_2CuO_4[b]	Eu_2CuO_4[b]
Space group	*I4/mmm*	*I4/mmm*

Lattice parameter (Å)	*a*=3.9048(3), *b*=3.9048(3), *c*=11.9149(3)	*a*=3.9043(3), *b*=3.9043(3), *c*=11.9136(3)
Atom	x, y, z	x, y, z
Eu	0.0000, 0.0000, 0.3495(3)	0.0000, 0.0000, 0.3507(3)
Cu	0.0000, 0.0000, 0.0000	0.0000, 0.0000, 0.0000
O1	0.0000, 0.5000, 0.0000	0.0000, 0.5000, 0.0000
O2	0.0000, 0.0000, 0.1734(3)	0.0000, 0.0000, 0.1711(3)
Phase 3	CuO	CuO
Space group	*C2/c*	*C2/c*
Lattice parameter(Å)	*a*=4.6939(3), *b*=3.4336(3), *c*=5.1326(3)	*a*=4.6930(3), *b*=3.4336(3), *c*=5.1329(3)
Atom	x, y, z	x, y, z
Cu	0.2500, 0.2500, 0.000	0.2500, 0.2500, 0.000
O	0.0000, 0.4181(3), 0.2500	0.0000, 0.4181(3), 0.2500
R factor[c]	R_{wp}=0.017,R_p=0.098	R_{wp}=0.027,R_p=0.014

[a] The occupancy of Cu/Mn is 0.316/0.684

[b]The atom coordination for Eu_2CuO_4 is referenced to $Sm_{2-x}Sr_xNiO_{4+\delta}$ with the same structure[1].

[c] R_p is sum($|I_0-I_C|$)/sum(I_0), and R_{wp} is weighted R factors for X-ray diffraction data.

2. The binding energies and ratio of Mn^{4+}:Mn^{3+} in the samples

Table S3 the binding energies and ratio of Mn^{4+}:Mn^{3+} in the samples

	***E*(Mn *2p*$_{3/2}$)/eV**	**FWHM (eV)**	***E*(Mn *2p*$_{3/2}$)/eV**	**FWHM (eV)**	**obtained Ratio of Mn^{4+}:Mn^{3+}**	**expected Ratio of Mn^{4+}:Mn^{3+}**
C1			641.9	2.9	0:100	0:100
C2	642.8	2.9	641.7	2.6	10:90	11:89
C3	642.8	2.5	641.7	2.5	26:74	25:75
C4	642.8	1.9	641.5	2.3	45:55	43:57

3. Table S4 The effective magnetic moments and Weiss constants of EuMn1-xCuxO$_{3-\delta}$ ($0 \leqslant x \leqslant 0.3$).

Sample	Curie constant (C)	μ_{exp} (μB)	θ (K)	μ_{cal} (μB)
C1	4.87	6.24	-84	5.96
C2	4.00	5.66	-27	5.71
C3	3.60	5.37	-14	5.27
C4	3.48	5.28	-18	5.15

4. Some additional discussions on the negative magnetization

In the manuscript, we have intended to believe that the negative values observed in the ZFC curves of our sample $EuMnO_3$ should be due to that the zero field in the cooling case is a small negative field. In order to confirm this, more measurements have been done.

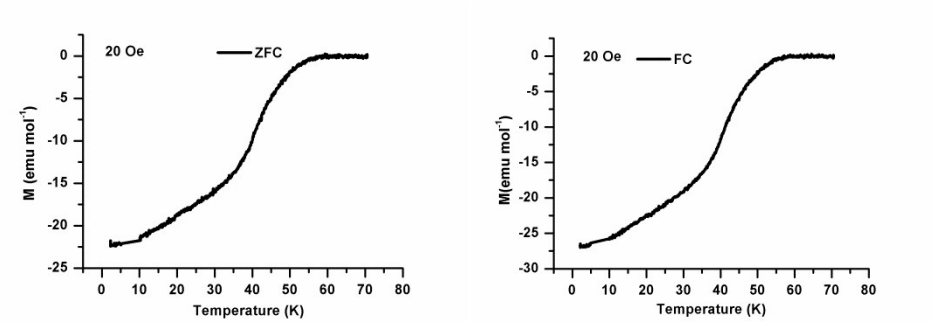

Figure S1 Temperature dependent magnetization of C1 measured at a field of 20 Oe

Figure S1 shows the ZFC (zero field cooling) and FC (field cooling) curves with the measured and cooling field about 20 Oe once. At this measurement, negative magnetizations are observed in both ZFC and FC case. We think this is caused by the fact that the measurement and cooling field at this case is really a negative field. Because when the field is increased to 40 Oe, the positive magnetization can be observed in FC case although the negative magnetization is still observed in ZFC case as shown in Fig.S2.

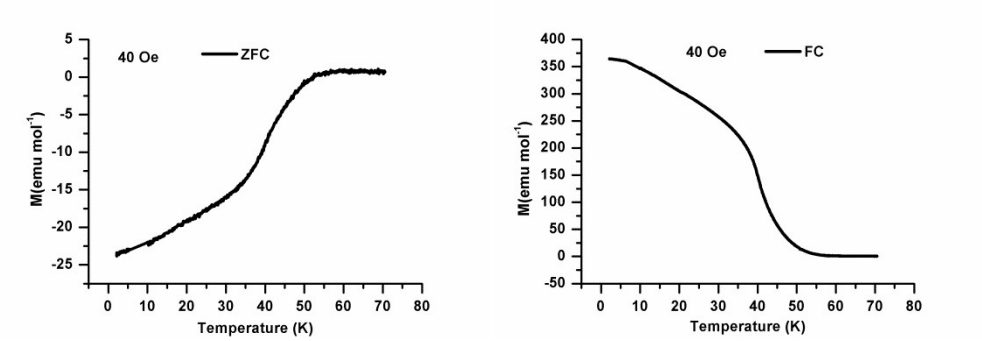

Figure S2 Temperature dependent magnetization of C1 measured at a field of 40 Oe.

When the field increases further to 100 Oe, negative magnetization is still observed in ZFC case. However, two peaks around 41K and 50K in the positive region can be observed, which are shown in Fig.S3.

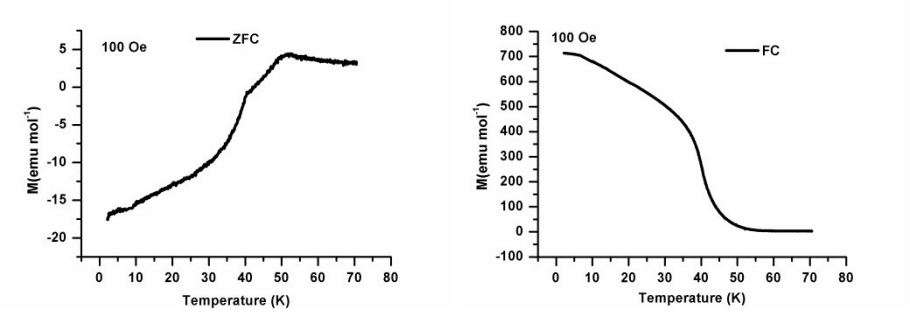

Figure S3 Temperature dependent magnetization of C1 measured at a field of 100 Oe.

When the field is about 500 Oe, negative magnetization can be observed in ZFC case only below 20K. The two peaks move to 41K and 47K in the positive region, and become clearer, which are shown in Fig.S4.

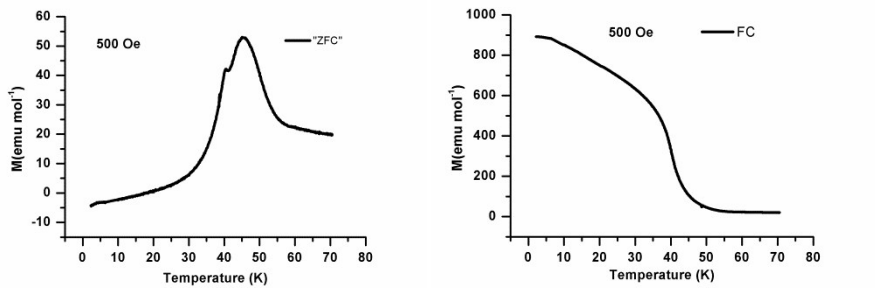

Figure S4 Temperature dependent magnetization of C1 measured at a field of 500 Oe.

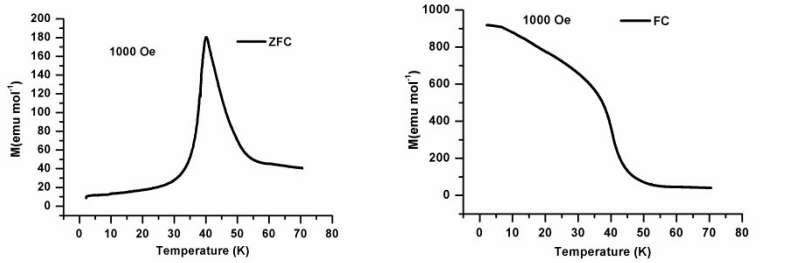

Figure S5 Temperature dependent magnetization of C1 measured at a field of 1000 Oe.

When the field is larger than 1000 Oe, no negative magnetization can be observed in ZFC case. One sharp peak appears at about 41K in the ZFC curve for the field of 1000 Oe, and a round peak around 35K appears in the ZFC curve for the field of 5000 Oe, which are shown in Fig.S5 and S6.

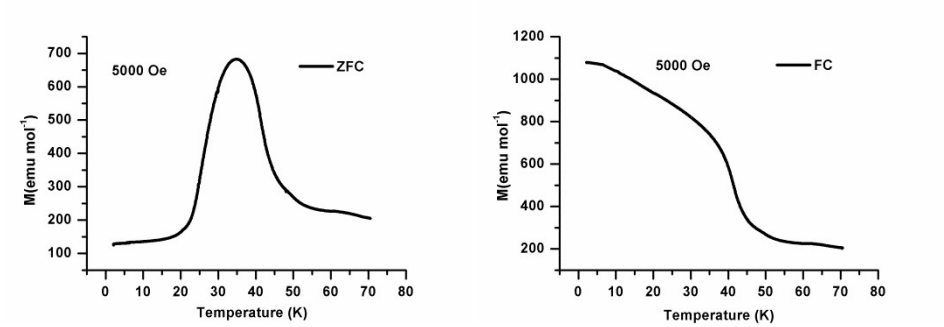

Figure S6 Temperature dependent magnetization of C1 measured at a field of 5000 Oe.

The above data is little different from that presented in the manuscript. In fact, the positive magnetization can be observed for the field of 20 Oe as shown in Figure S7, although it is rare.

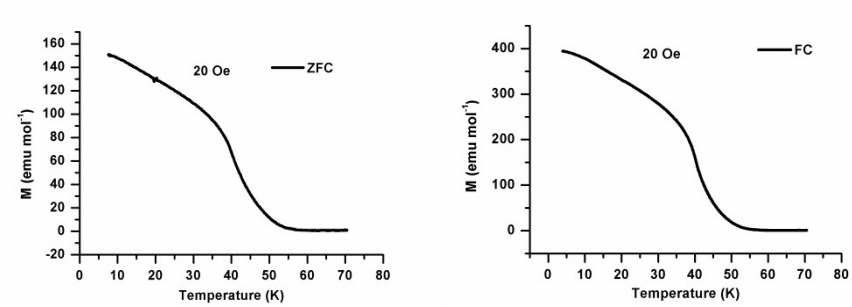

Figure S7 Temperature dependent magnetization of C1 measured at a field of 20 Oe

5. Some efforts on the magnetic structure of $EuMnO_3$

It is not lucky that the magnetic structure of $EuMnO_3$ is unsolved until now. We have planned to solve the magnetic structure using neutron diffraction data at low temperature. It is found that it is very hard to get the neutron diffraction data for $EuMnO_3$ because the neutron can be absorbed by Eu. With the help of Dr M. Avdeev at the OPAL facility, the neutron diffraction data of $EuMnO_3$ have been obtained and shown in Fig.S8. The magnetic reflections can be observed at 3K around 12.2° shown in Fig.S8. However, the quality of the data is not good enough for solving the magnetic structure. We are planning to get ^{153}Eu to synthesize $^{153}EuMnO_3$ to recollect the neutron diffraction data for solving the magnetic structure. At present, we just compared our results to the similar results published on the literatures to help the reader have a comparable memory of our results.

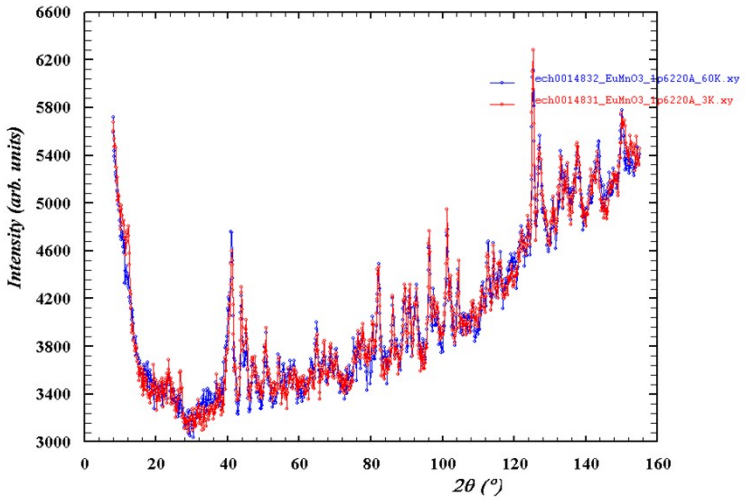

Figure S8 Neutron diffraction data obtained at 3 (Red) and 60K (blue) for $EuMnO_3$

6. Some efforts to find the low temperature magnetic anomaly of $EuMnO_3$ from Arrot plots

We have tried our best to analyze the Arrot plots of our samples to find the low temperature magnetic anomaly. This plot is mainly used for paramagnetic to ferromagnetic phase transition. In such plots, H/M versus M^2 should go as $H/M=a(T-T_C)+bM^2+cM^4+\ldots$ at values of H. At T_C, the intercept changes sign. As suggested by S.K. Baerjee (Phys. Lett. 1864, 12, 16), b is positive for second order transitions and is negative for first order transition. The typical initial magnetization isotherms are presented in Fig.S9a (J. Mira, J. Rivas, F. Rivadulla, C. Vázquez-Vázquez, and M. A. López-Quintela, Phys. Rev. B 1999, 60, 2998), from which the Arrot plot can be drawn as shown in Fig.S9b.

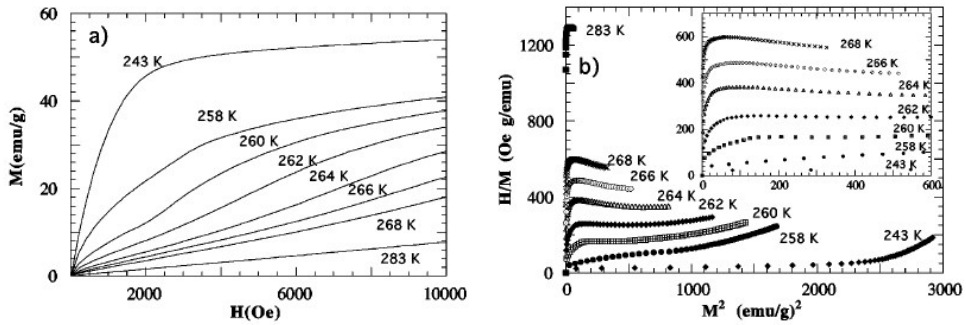

Figure S9 a) Magnetization versus magnetic field isotherms for $La_{2/3}Ca_{1/3}MnO_3$ in the vicinity of its T_C . b) H/M vs M^2 plot of the above isotherms. It is clear the negative sign of the slope for some temperatures. The inset shows the detail for small values of M^2. The figure is from J. Mira, J. Rivas, F. Rivadulla, C. Vázquez-Vázquez, and M. A. López-Quintela, Phys. Rev. B 1999, 60, 2998.

The initial magnetization isotherms of C1 ($EuMnO_3$) are shown in Fig.R5a. They are very different from the typical ones shown in Fig.S9. The reason may be that $EuMnO_3$ is canted anti-ferromagnetic ordering at low temperature. The corresponding Arrott plots are shown in Fig.S10b. They are different from the typical ones shown in Fig.S9. At present, we think this phenomenon may be related to that $EuMnO_3$ is canted antiferromagnetic ordered. More detail studies are undertaking. As mentioned in the answer for the first comment, we are trying our best to perform neutron diffraction for $^{153}EuMnO_3$ to solve the magnetic structure at low temperature. Then it may be possible to check if Eu provides certain low temperature magnetic anomaly,

which does not be found from the present data. Any suggestions and helps are welcome.

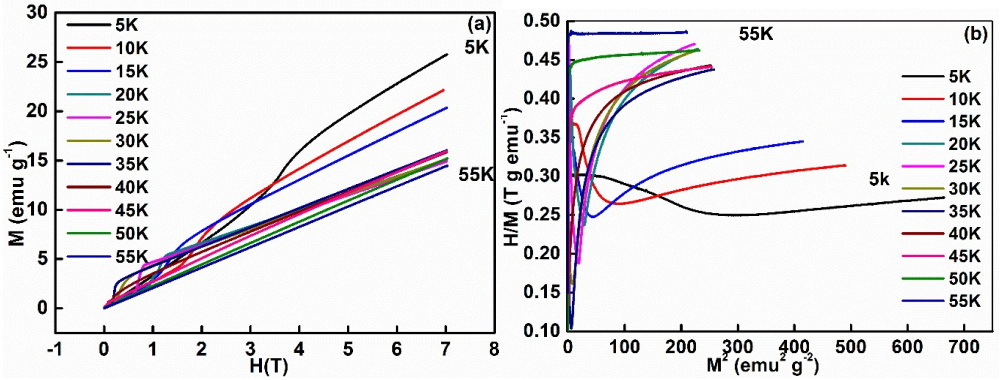

Figure S10 a) Magnetization versus magnetic field isotherms for C1 ($EuMnO_3$). b) H/M vs M^2 plot of the above isotherms.

Reference

1. H. Lou, Y. P. Ge, P. Chen, M. H. Mei, F. T. Ma, G. L. Lü, *J. Mater. Chem.* 1997, 7, 2097.